A Three Dimensional Model for Selective Laser Sintering

Ming-shen M. Sun, Joseph J. Beaman
The University of Texas at Austin

Abstract

A three-dimensional model for Selective Laser Sintering is derived based on the basic model structure: optical-thermal-rheological submodels. Combining these submodels, a three-dimensional simulation is developed which is an extension of a previously developed one-dimensional model. This model can be used to calculate important process properties that effect the quality of sintering such as sintering depth, thermal stress, and edge definition. *Key words: model, sintering.*

I. Introduction

Selective Laser Sintering is a newly developed manufacturing technique which uses a laser to sinter material powder selectively to produce three dimensional mechanical parts. The physical process associated with this process includes: laser absorption, heat transfer, and sintering of powder. An integrated model describing these behaviors has been proposed by the author [1], this model consists of an optical submodel, a thermal submodel and a sintering submodel. A one dimensional simulation program has been previously developed. A comparison between the computer simulated sintering depth and the real sintering depth shows that this model successfully describes the laser sintering behavior. Further refinement of this model is presented in this paper. Detail theory of each of the submodels is discussed. All the submodels will be supported by theory and partially tested by experiments. A three-dimensional simulation program based on the refined model is implemented. Output of this program will provide useful information on the sintering behavior such as the temperature distribution or the relative density distribution in the three dimensional powder bed. This information could be used to calculate other important properties that affect the sintering qualities such as the sintering depth, edge definition or the thermal stress field in the powder bed.

Schematic illustration of the Selective Laser Sintering process is shown in fig.1.

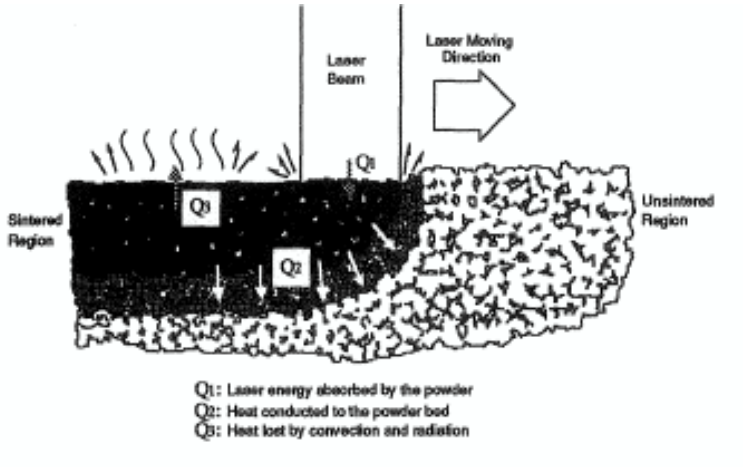

Figure 1. The Selective Laser Sintering process

II. Optical Submodel

Consider a laser light of intensity I_o shining on the surface of a powder bed which can be treated as a semi-transparant absorbing medium, the intensity distribution of the penetrated light within the powder bed is

$$I(z) = (1-R)\, I_o \exp(-\beta z) \tag{1}$$

Important optical properties include surface reflectivity R and extinction coefficient β, these properties are functions of refraction index of the material at a laser wavelength and geometry of the powder bed.

Surface reflectivity for light traveling from a non-absorbing medium (refraction index n_1) into an absorbing one (complex refraction index $n_2=n_2'+n_2''i$) with an incident angle ϕ is given in [2] as

$$R = \frac{1}{2}\frac{M + x^2 - x[2(M+L)]^{1/2}}{M + x^2 - x[2(M+L)]^{1/2}} + \frac{1}{2}\frac{M + P^2 x^2 - x(M+y^2)[2(M+L)]^{1/2}}{M + P^2 x^2 - x(M+y^2)[2(M+L)]^{1/2}} \tag{2}$$

where $x = \cos\phi$, $y = \sin\phi$, $M^2 = L^2 + 2(\mu'\mu'')^2$, $P = \mu'^2 + \mu''^2$, $L = \mu'^2 - \mu''^2 - y^2$, $\mu' = n_2'/n_1$, and $\mu'' = n_2''/n_1$. Shown in figure 2 is the spectral absorptivity $(1-R(\phi))$ for $n_1=1$(air) and $n_2=1.5+n_2''i$ with n_2'' ranging from 0 to 10.

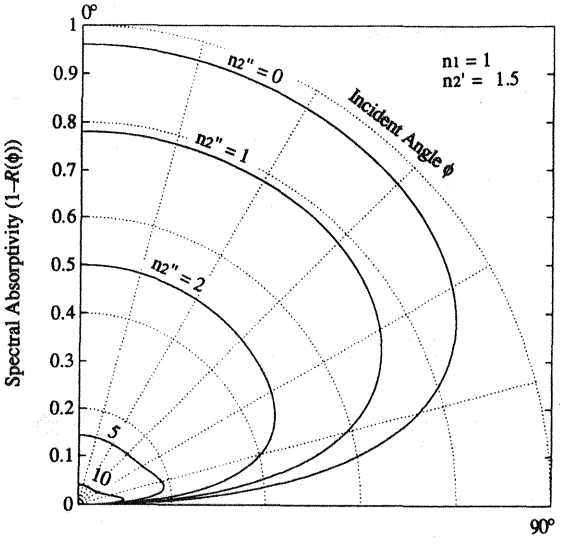

Figure 2. The spectral absorptivity of material $n_2=1.5+n_2''i$

If the geometry of the powder bed is known, the incident angle ϕ of parallel light beams with respect to the local surface normal can be described as a function of position, and the overall effective surface absorptivity can integrated. The calculated effective surface absorption for a single sphere, a cubic pack bed and a close pack bed of material with refraction index $n_2=1.5+n_2''i$ is shown in figure 3. In the calculation, the beam entering the pore between particles is assumed trapped in the pore, therefore the absorptivity of that area is 1.0.

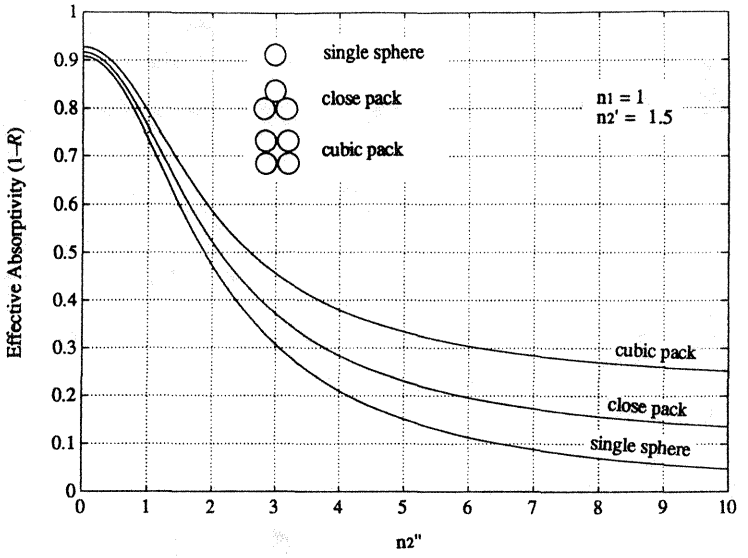

Figure 3. The effective surface absorptivity of some powder beds

The second optical property in equation (1) is the extinction coefficient β. Due to geometric complexity of a powder bed structure, it is very difficult to come up with an exact formula for β. However, it is not difficult to imagine that the extinction distance $1/\beta$ for a highly opaque material will be of the same order of magnitude as the particle size, because the decay of light intensity within a powder bed is mainly due to the blocking of light by the particles.

The optical submodel is constructed by measuring the refractive index n_2', n_2'' of the material, assuming a powder bed geometry to calculate R, and by assuming that $1/\beta =$ particle size. An optical experiment to measure R and β such as an integrating sphere technique is needed to test this model [3-4].

III. Thermal Submodel

The heat transfer behavior in the powder bed can be described by the conduction equation:

$$\rho C \frac{\partial T}{\partial t} = \nabla(k \nabla T) + g(x,y,z,t) \tag{3}$$

where ρ, C, k are the apparent density, specific heat and thermal conductivity of the powder bed, and $g(x,y,z,t)$ is a internal heat source function due to the penetrating laser light. For a moving Gaussian beam whose intensity decays as described in eq.(1), the heat source function is:

$$g(x,y,z,t) = (1-R)\beta I_o \exp\left[-\frac{(x-v_x t)^2+(y-v_y t)^2}{w^2} - \beta z\right] \tag{4}$$

where v_x and v_y are the beam velocity in the x and y direction, w is the radius of the Gaussian beam.

The conduction equation (3) is subject to two boundary conditions:
(1) At the top surface of the powder, heat is lost due to convection and radiation:

$$-k\frac{\partial T}{\partial z}|_{z=0} = h\,(T_a - T_{z=0}) + \varepsilon\sigma\,(T_e^4 - T^4_{z=0}) \tag{5}$$

where h is the convection coefficient, T_a is the air temperature, ε is the surface emissivity of the powder bed, T_e is the surface temperature of the environment enclosing the powder bed. (2). At the bottom of the powder bed (infinite depth), no heat is lost.

$$-k\frac{\partial T}{\partial z}|_{z=\infty} = 0 \tag{6}$$

In contrast to the conduction problem of a solid material, the thermal conductivity of a powder bed can vary from position to position depending on the local temperature as well as the condition of contact between particles and the local porosity. Yagi and Kunni[5] have formulated a model for effective conductivity of a packed bed considering the conduction, convection and radiation effect within a powder bed, their result is

$$k_e = \frac{\rho k_s}{1+\phi k_s/k_g} \tag{7}$$

where k_s is conductivity of the solid material, k_g is the conductivity of air, ρ is the solid fraction, and ϕ is an empirical coefficient = $0.02x10^{2(0.7-\rho)}$.

An empirical model has also been developed by Xue[6] especially for the Selective Laser Sintering powder as

$$k_e = \left(6.3 + 22\sqrt{0.09k_s - 0.016}\right)\frac{\rho k_s}{\frac{k_s}{k_g(1-\rho)^{0.75}} - 1} \tag{8}$$

Using one of these models, temperature field in the powder bed can then be solve by integrating equation (3) using a numerical method.

IV. Sintering Submodel

A model describing sintering behavior of viscous porous structure has been derived by Scherer[7-9]. Although it was found that this model does not exactly explain behavior of Selective Laser Sintering, it provides a good example of derivation of a sintering model. Based on a cubic pack powder bed geometry and by introducing a factor: fraction of sintering ζ, One author[Sun] has developed a model for a sintering powder bed[10] with sintering rate equations

$$\dot{x} = -\frac{\pi\gamma a^2}{6\eta_b x^3}\left\{r - (1-\zeta)x + \left[x - (\zeta + \frac{1}{3})r\right]\frac{9(x^2-r^2)}{18rx-12r^2}\right\} \tag{9}$$

where a is the original radius of the power particle, x and r are geometry of a cubic pack structure that satisfy

$$3x^3 - 9r^2x + 4r^3 + 2a^3 = 0 \tag{10}$$

Relative density of a powder bed is

$$\rho = \frac{\pi a^3}{6x^3} \tag{11}$$

and bulk viscosity of a porous powder bed is given by [11]

$$\eta_b = \frac{4\eta\rho^3}{3(1-\rho)} \tag{12}$$

For an amorphous material such as most polymers, viscosity η is a function of temperature in Arrhenius form

$$\eta = \eta_o \exp\left(\frac{\Delta E}{RT}\right) \tag{13}$$

where ΔE is the activation energy of the material.

By knowing the temperature at a position in the powder bed, the local viscosity and sintering rate can be calculated. Density change can be calculated from the sintering rate equation (9).

V. The Computer Simulation

Combining the three submodels discussed above, a three-dimensional computer simulation program has been developed. This program use several three dimensional arrays to record the temperature, relative density and thermal properties of the given powder bed. The inter-relationship between properties are described by finite difference equation derived from equations (1) to (13). Input variables to this program are:

1. Dimensions of the powder bed, numbers of grid points in three directions, time step and time to record the data. Direction and position of recorded data array.
2. The laser properties: laser intensity I_o, Gaussian beam e radius w, beam velocity v_x, v_y, and initial position (x_o,y_o).
3. Optical properties: refraction index n_2' and n_2'', packing geometry, particle size $2a$, extinction coefficient β.
4. Thermal properties: k_s, k_a, convection and radiation conditions h, ε, T_a, T_e, and the initial powder bed temperature T_o.
5. Rheological properties μ_o, ΔE, surface tension γ.

An example of simulation output: the temperature and relative density distribution are shown in figures 4 and 5.

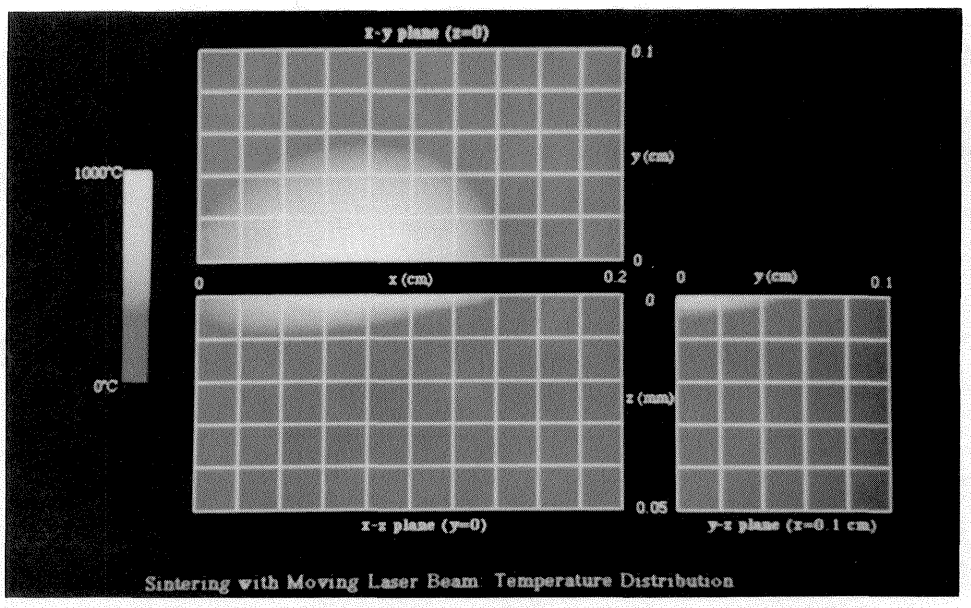

Figure 4. Temperature rise in the powder bed calculated by the 3-D simulation program

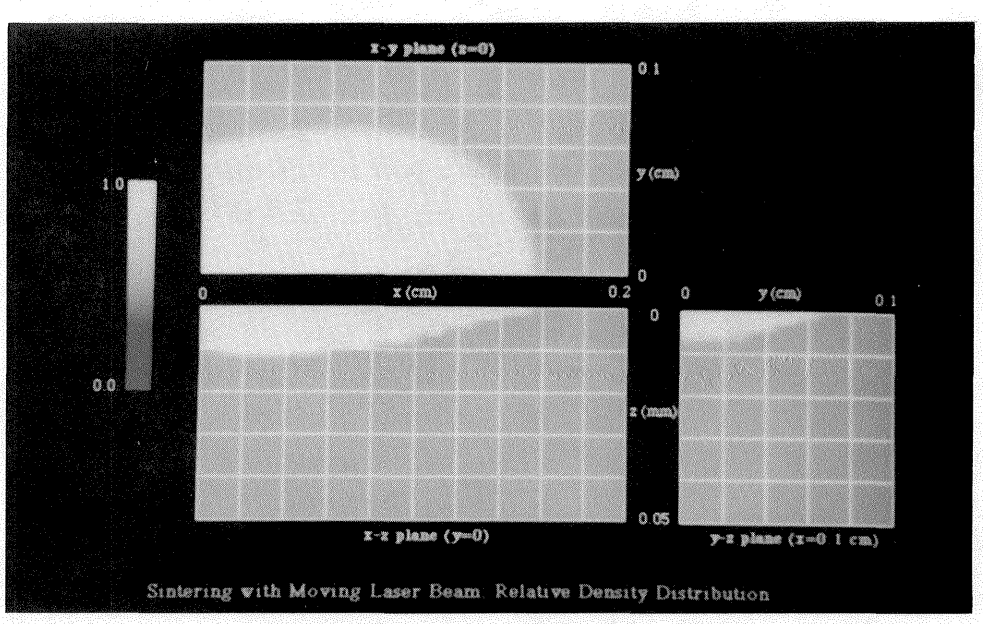

Figure 5. Relative density of the powder bed calculated by the 3-D simulation program

V. Analysis of the Simulation Result

Very similar to the 1-D simulation result, the result of the 3-D simulation shows a steep change in bed density from the unsintered region to the sintered region, and a very uniform density in the sintered region, a distinct sintering front is observed moving and stopping in the powder bed as the laser is scanned. As discussed in the previous research [1], the sintering depth is an useful qualifier of the sintering. Given a powder with known properties and geometry, running the simulation with varied laser control parameters: the laser power intensity and the scanning speed, the sintering properties can be established from the sintering depth plot. An example is shown in figures 6 and 7. The threshold

power and the maximum scanning speed to get sintering can be estimated from these plots. A surface plot can also be constructed in the power-speed space from which an simplified relation can be derived. This simplified model will be useful in Selective Laser Sintering process control such as to determine the optimal laser parameters given that sintering depth is larger than the thickness of one powder layer.

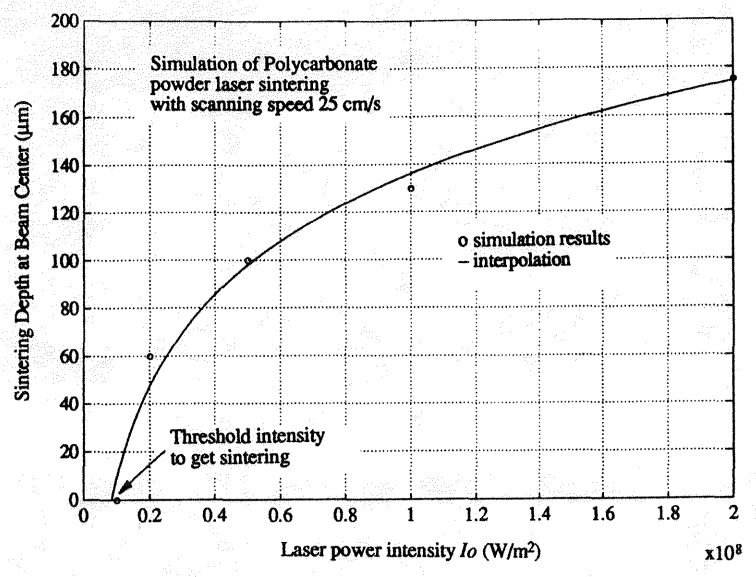

Figure 6. The relation between sintering depth at beam center and laser power intensity

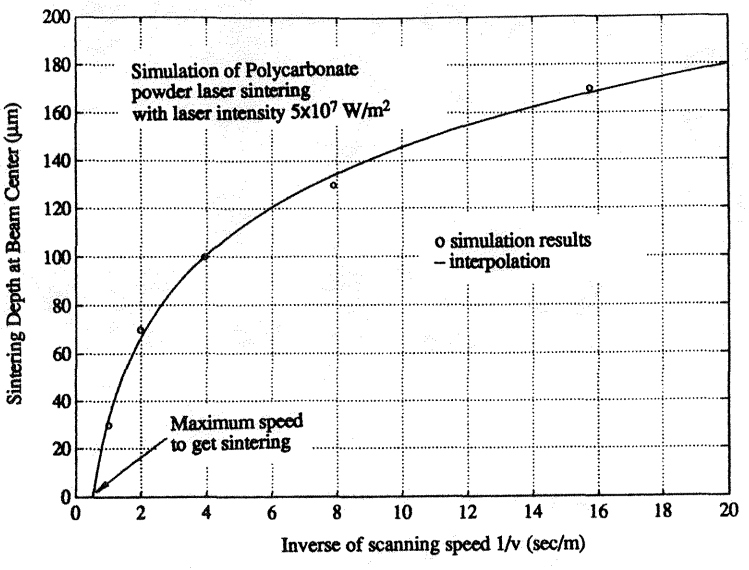

Figure 7. The relation between sintering depth at beam center and laser scanning speed

Other than sintering depth, simulation results can also provide the information about the sintering quality such as: absolute density value in the sintered region. The distribution of sintered density near the sintered boundary indicate the edge definition. The temperature distribution within the powder bed tells us how uneven the temperature in the bed is which can cause a thermal stress problem.

VI. Summary

A three-dimensional model for Selective Laser Sintering is derived based on the basic model structure: optical-thermal-rheological submodels. Combining these submodels, a three-dimensional simulation program is developed. With material properties and the laser control parameters as inputs, temperature and density distribution of a powder bed can be calculated. These data can provide useful information about the sintering properties such as the sintering depth or the part definition. A simplified relation between sintering depth and laser control parameters will be important in sintering process control, which can be derived from the extensive simulation results. Future goal of this work is to explore more experimental data on properties of material to support each submodel such as optical property test, adjust the integrated model for experimental consistency, and build relation between sintering depth and the laser control parameters.

References:

1. Sun, M., Beaman, J., Barlow,J., *"Parametric Analysis of the Selective Laser Sintering Process,"* SFF Symposium, , Austin, TX (1990).
2. Meeten, G., *"Optical Properties of Polymers,"*p14-17, Elsevier Appl. Sci. Publishers, New York (1986).
3. Gindele, K., Kohl, M., Mast, M., *"Spectral Reflectance Measurements Using an Integrating Sphere in the Infrared,"* Applied Optics, **24** [12], 1757-60 (1985).
4. Kessek, J., *"Transmittance Measurements in the Integrating Sphere,"* Applied Optics, **25** [16], 2752-6 (1986).
5. Yagi,S., Kunni, D., *"Studies on Effective Thermal Conductivities in Packed Beds,"* J AIChe. **3**, [3], 373-81 (1989).
6. Xue, S., Barlow, J., *"Models for Prediction of the Thermal Conductivities of Powder,"* SFF Symposium, Austin, TX (1991).
7. Scherer, G., *"Sintering of Low-Density Glasses: I, Theory,"* J. Am. Cer. Soc. **60** [5-6] 236-9 (1977).
8. Scherer, G., *"Sintering of Low-Density Glasses: II, Experimental Study,"* J. Am. Cer. Soc. **60** [5-6] 239-45 (1977).
9. Scherer, G., *"Sintering of Low-Density Glasses: III, Effect of a Distribution of Pore Size,"* J. Am. Cer. Soc. **60** [5-6] 245-8 (1977).
10. Sun, M., *"A Model for Partial Viscous Sintering,"*SFF Symposium, Austin TX (1991).
11. Bordia,R., Scherer, G., *"On Constrained Sinteing-II. Comparison of Constitutive Models,"* Acta matall. **36** [9] 2399-409 (1988).